Edge Modelling for W7-X

R. Schneider, M. Borchardt, J. Riemann, X. Bonnin,
J. Nührenberg, A. Mutzke
Max-Planck-Institut für Plasmaphysik, EURATOM Association,
D-17491 Greifswald
e-mail contact of main author: Ralf.Schneider@ipp.mpg.de

Abstract. The edge modelling activities for W7-X are summarized. The status of the new 3D SOL transport code BoRiS is presented, including an algorithm for calculation of magnetic coordinates and metric coefficients. In addition, the analysis of a toroidally averaged island topology with respect to the effect of drift and currents is discussed using the 2D B2-solps5.0 code.

1. 3D Modelling with BoRiS

For the W7-X stellarator a divertor is planned using the existing island topology of the magnetic field, where configurations with and without strong stochastic effects are possible. The latter case is of particular interest when comparing stellarator and tokamak results.
BoRiS is a new 3D SOL transport code aimed at solving a system of plasma fluid equations like the well-known B2 code. In order to deal with the complex 3D geometry of W7-X, BoRiS uses magnetic coordinates, thus allowing for standard discretization methods with higher-order schemes retaining full geometric flexibility.

Having started with a system of simplified energy equations [1, 2] for the electrons and ions consisting of two anisotropic Laplace equations being coupled by a heat exchange term, the actual physics model of BoRiS is currently extended by including the equations for the parallel momentum and the plasma density, leading to the following system:

$$\frac{\partial n_i}{\partial t} + \nabla_{\shortparallel}\big(n_i \vec{u}_{\shortparallel}\big) - \nabla_{\perp}\big(D_{\perp}\nabla_{\perp} n_i\big) = S_n^i$$

$$\frac{\partial}{\partial t}\big(m_i n_i \vec{u}_{\shortparallel}\big) + \nabla_{\shortparallel}\big(m_i n_i u_{\shortparallel}^2\big) - \nabla_{\perp}\big(m_i \vec{u}_{\shortparallel} D_{\perp}\nabla_{\perp} n_i\big) = -\nabla_{\shortparallel}\big(p_e + p_i - \eta_{\shortparallel}\nabla_{\shortparallel} u_{\shortparallel}\big)$$

$$\frac{\partial}{\partial t}\big(\tfrac{3}{2}p_e\big) + \nabla_{\shortparallel}\big(\tfrac{5}{2}T_e\, n_i \vec{u}_{\shortparallel} - \kappa_{\shortparallel}^e \nabla_{\shortparallel} T_e\big) + \\ + \nabla_{\perp}\big(-\tfrac{5}{2}T_e\, D_{\perp}\nabla_{\perp} n_i - \kappa_{\perp}^e \nabla_{\perp} T_e\big) = -\big(\vec{u}_{\shortparallel}\nabla_{\shortparallel} p_e - Q_{ei}\big)$$

$$\frac{\partial}{\partial t}\big(\tfrac{3}{2}p_i + \tfrac{1}{2}m_i n_i \vec{u}_{\shortparallel}^2\big) + \nabla_{\shortparallel}\big(\tfrac{5}{2}T_i\, n_i \vec{u}_{\shortparallel} - \kappa_{\shortparallel}^i \nabla_{\shortparallel} T_i\big) + \\ + \nabla_{\perp}\big(-\tfrac{5}{2}T_i\, D_{\perp}\nabla_{\perp} n_i - \kappa_{\perp}^i \nabla_{\perp} T_i\big) = \big(\vec{u}_{\shortparallel}\nabla_{\shortparallel} p_e - Q_{ei}\big),$$

Here we have the ion density $n_i = n_e$, the parallel velocity $u_{\shortparallel}$ (with $\vec{u} = \vec{u}_{\shortparallel} + \vec{u}_{\perp} = \vec{u}_{\shortparallel} - D_{\perp}\nabla_{\perp} n_i/n_i$), the temperatures $T_{e,i}$, the parallel and perpendicular conductivities

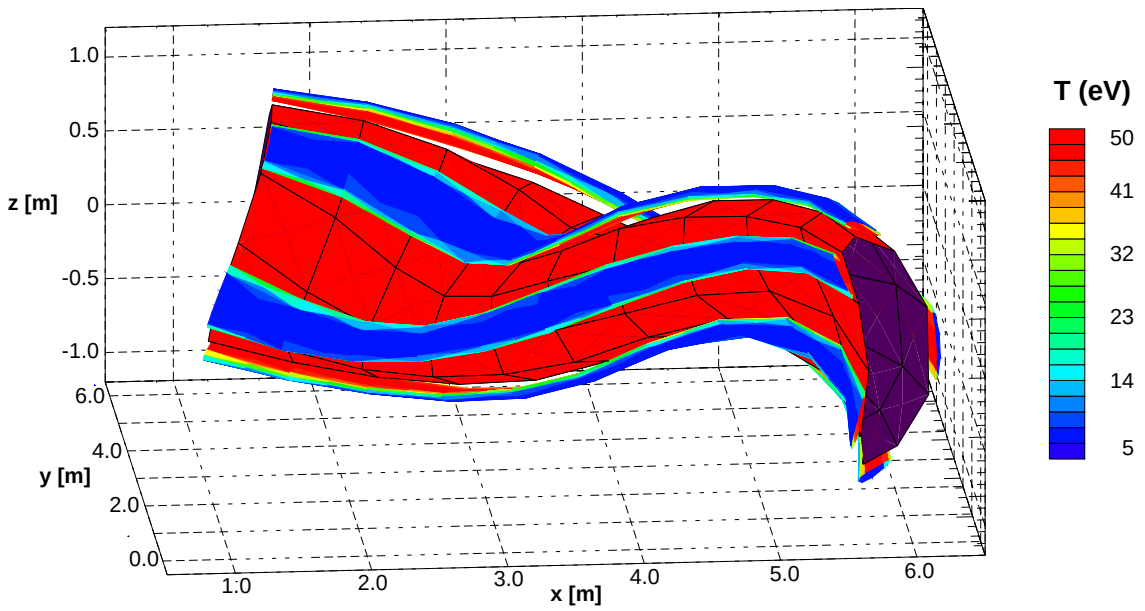

FIG. 1: Island flux tubes with electron temperature profiles in real space.

$\kappa_{\|}^{e,i}$ and $\kappa_{\perp}^{e,i}$, an anomalous diffusivity $D_{\perp}$, the heat exchange term Q_{ei} and a source term S_{n_i}.

1.1. Continuity equation tests

In implementing the new equations, we performed several tests in different geometries. A simple slab model can be used to test basic properties and different contributions. On the other hand, the equations can also be solved serving as a diagnostic tool for the specifics of the actual 3D geometry [3].
As an example, the continuity equation was solved in a W7-X geometry assuming the absence of sources and a spatially constant test-velocity field $\vec{u} = (u_{\|}, u_{\perp 1}, u_{\perp 2})$. Using different components of the test-velocity, the metric properties of the computational domain were probed, thus yielding a fingerprint of the geometry.

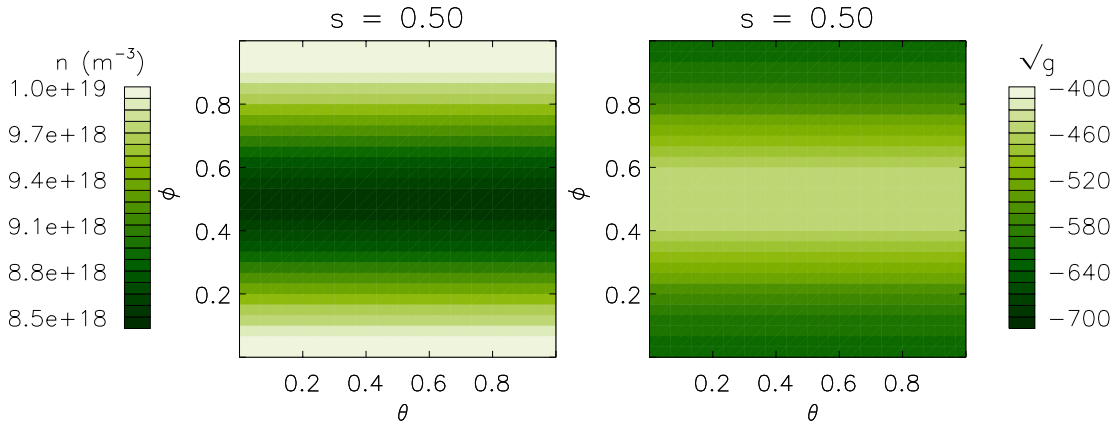

FIG. 2: Density profile (left) and metric coefficient $\sqrt{g}$ (right).

Fig.2 shows the density profile $n(s = \text{const})$ as obtained with a velocity field $\vec{u} = (u_{\|}, 0, 0)$

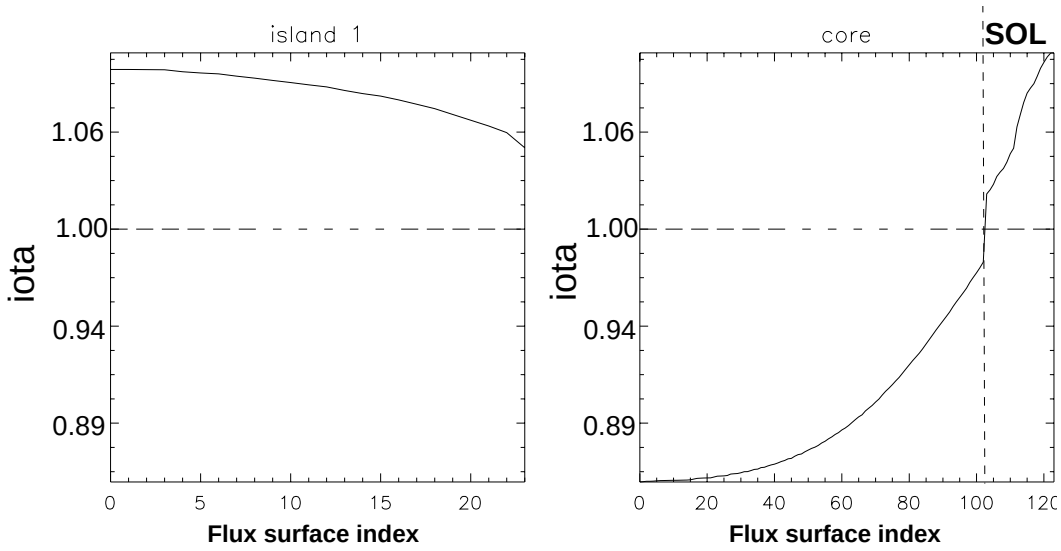

FIG. 3: Iota as a function of the radial flux surface index for the three plasma regions

in comparison to the metric coefficient $\sqrt{g}$ which acts as a weight factor on the interfaces between computational cells. Since $\vec{u}$ is parallel to the magnetic field there is only a 1D variation along the toroidal coordinate ϕ.

1.2. Magnetic coordinates

The solution of the 3D transport equations in magnetic coordinates requires good knowledge of the spatially-varying metric coefficients, in particular near the island chain boundary in the W7-X edge that BoRiS must resolve. The current MHD codes do not appropriately treat such separatrix regions when computing metric coefficients, thus we have developed a new method for their evaluation. This method assumes only the existence of magnetic surfaces (so zero ergodicity) and knowledge of the magnetic field (and its derivatives) in the region of interest. We first identify the X- and O-points of the field by finding where the field lines close upon themselves after only one toroidal turn. Then, for each topological region (plasma core, islands, SOL), we follow field lines long enough to describe the magnetic surfaces to the desired accuracy (typically 400 toroidal turns). On these surfaces, we can now compute the rotational transform ι (FIG. 3), the toroidal flux F_T, and the poloidal and toroidal currents I and J. To proceed further, we make use of an algorithm developed by Nemov [4] which allows one to reduce the computation of gradients to initial value problems necessitating only integration along the field lines. By so doing, we can obtain numerical expressions for the Clebsch components of the field $\nabla\psi$ and $(\nabla\theta - \iota\nabla\zeta)$ in each plasma region. The metric coefficients are then trivially obtained. The determination of the Nemov initial conditions requires the radial derivative $\partial F_T/\partial R$, which is the only radial derivative appearing. Since all integrations are done along field lines, this method provides the desired numerical accuracy for our purposes.

2. The plasma edge in the presence of a diverted island

In parallel to the development of the full 3D code we try to use the existing complex

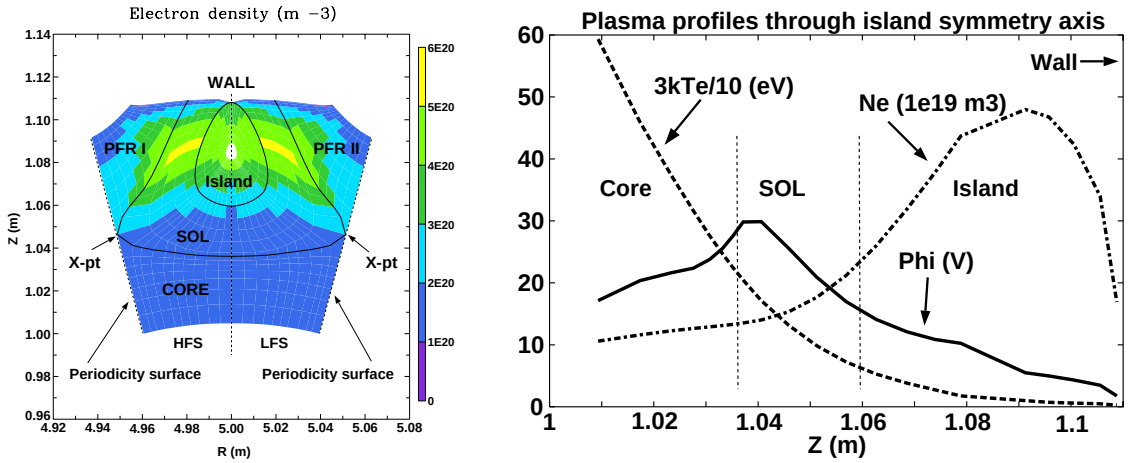

FIG. 4: Typical density distribution (left) obtained for a no-drifts high-recycling case (HFS: High-field side; LFS: Low-field side). The island, core, SOL and private flux regions (PFR I and II), their boundaries, X-points and periodicity surfaces are also shown. The dashed line shows the cut used for the 1-D temperature (dashed line), density (dot-dashed line) and electric potential (solid line) profiles along the symmetry line at $R = 5.00$ m (right). Note the clear potential maximum just outside the separatrix, the density accumulation inside the island and the scale difference between $3kT_e$ and ϕ.

2D codes for specific studies of problems characterized by the island divertor topology. Therefore, the B2-solps5.0 edge plasma multifluid code was extented for the analysis of the electric potential and electric field in an island divertor configuration to handle such cases using a toroidally averaged grid to represent the magnetic geometry. Here, the usual set of fluid conservation equations (particles, momentum, energy) as well as the electric potential equation (current continuity) are solved [5, 6].

Of special interest here, beyond the addition of the electric potential equation, are the diamagnetic and parallel viscosity terms, as well as the $\mathbf{E} \times \mathbf{B}$ drift, none of which were included in previous island divertor simulations [7, 8, 9]. A neutral fluid model accounts for recycling and ionization effects. A more accurate representation of the neutrals would require a 3-D simulation because of the complex plasma geometry. Although full 3-D models of stellarator plasma edge transport are becoming available [10, 3], they do not yet treat self-consistently the electric potential, or contain drifts and currents [9]. It is thus useful to obtain knowledge about the electric field structure of island divertors using our current 2-D tokamak simulation tools. We begin by presenting results of simulations involving no drift terms, so as to establish a reference case. Diamagnetic and parallel viscosity terms are then added, and their influence described. Finally, we discuss the further impact of the $\mathbf{E} \times \mathbf{B}$ terms.

The dominating feature of these plasma configurations is particle accumulation inside the island [7]. In that sense, the island divertor behaves very differently from a standard tokamak divertor. We show the density distribution for a typical high-recycling case in FIG. 4. A density "pillow" across the island and SOL regions is readily apparent. For this run, we have chosen $n_e^{core} = 10^{20} m^{-3}$ and a heat flux through the core boundary of 220 kW as our boundary conditions (corresponding to 1.1 MW of SOL power influx for the complete 5-island system in W7-X). Out of these 220 kW, only about 20 kW reach the plates, and the remaining 200 kW are lost to radiation and ionization of the recycled

neutrals, of which 50 kW are dissipated inside the island region. Analysis of the particle flows shows that many recycled neutrals penetrate into the island and are ionized there, thus creating a density increase in and about the island region. The potential profile favors this density distribution by adopting a maximum near the separatrix and in general being very different from the values given by the simple $\phi = 3kT$ ansatz.

Concurrently, current loops get established which interconnect the SOL and the island region, but do not cross into the core plasma. Mirroring current flow loops also exist in both the core and the side private flux regions. As explained in [7], the "pillow" density depends strongly on the recycling conditions (in FIG. 4 we use a 99% recycling coefficient). Since the true geometry of the island is 3-dimensional and the plates are not toroidally continuous, our 2-dimensional simulations (with toroidally continuous plates) will overestimate the density accumulation. When we correct for this over-estimation by lowering the recycling coefficient, the island density accumulation rapidly disappears, while the current loops in the SOL become narrower, eventually failing to cross over into the island region.

Under the influence of the $\mathbf{E} \times \mathbf{B}$ drift these current loops grow lopsided, but are practically destroyed by diamagnetic effects. Concurrently, the island density accumulation is significantly reduced with the inclusion of drift effects.

References

[1] Borchardt, M. et al., EPS Conference, ECA 23J (1999) 1501, Maastricht

[2] Schneider, R. et al., Contrib. Plasma Phys. 40 (2000) 340

[3] M. Borchardt, J. Riemann, R. Schneider et al., J. Nucl. Mater. (2001), in press

[4] Nemov, V. V., Nuclear Fusion 28 (1988) 1727

[5] V. Rozhansky, S. Voskoboynikov, E. Kovaltsova et al., Contrib. Plasma Phys. 40 (2000) 423–430.

[6] R. Schneider, D. Coster, B. Braams et al., Contrib. Plasma Phys. 40 (2000) 328–333.

[7] F. Sardei, Y. Feng, P. Grigull et al., J. Nucl. Mater. 241–243 (1997) 135–148.

[8] G. Herre, P. Grigull and R. Schneider, J. Nucl. Mater. 266–269 (1999) 1015–1019.

[9] Y. Feng, G. Herre, P. Grigull et al., Plasma Phys. Control. Fusion 40 (1998) 371–380.

[10] Y. Feng, F. Sardei and J. Kisslinger, J. Nucl. Mater. 266–269 (1999) 812–818.